南京航空航天大学

论文集

（二〇〇八年）　第42册

高新院

南京航空航天大学科技部编

二〇〇九年五月

高 新 院

高新技术研究院2008年发表论文目录

序号	作者姓名	职称	单位	论文题目	刊物名称	年卷期
1	戴意涛 郭万林	博士 教授	高新院	Ultrahigh Frequency Longitudinal Oscillators from Single-Walled Carbon Nanotubes	Journal of Computational and Theoretical Nanoscience	2008, 5
2	戴意涛 郭万林	博士 教授	高新院	Simulation Studies of a "Nanogun" Based on Carbon Nanotubes	Nano Research	2008, 1
3	姜燕 郭万林	博士 教授	高新院	Convex and concave nanodots and lines induced on HOPG surfaces by AFM voltages in ambient air	Nanotechnology	2008, 19
4	李海军 郭万林	博士 教授	高新院	Transversely isotropic elastic properties of single-walled carbon nanotubes by a rectangular beam model for the C-C bonds	Journal of Applied Physics	2008, 103
5	钟文宇 郭万林	博士后 教授	高新院	Intrinsic aqueduct orifices facilitate K+ channel gating	FEBS Letters	2008, 582
6	马少杰 郭万林	博士 教授	高新院	Size-dependent polarizabilities of finite-length single-walled carbon nanotubes	Physics Letters A	2008, 372
7	石冶金 郭万林	硕士 教授	高新院	Relevance of Timoshenko-beam model to microtubules of low shear modulus	Physica E	2008, 41
8	台国安 郭万林	博士 教授	高新院	Hydrothermal synthesis and thermoelectric transport properties of uniform single-crystalline pearl-necklace-shaped PbTe nanowires	Crystal Growth & Design	2008, 8, 8
9	台国安 郭万林	博士 教授	高新院	Structural characterization and thermoelectric transport properties of uniform single-crystalline lead telluride nanowires	Journal of Physical Chemistry C	2008, 112, 30
10	台国安 郭万林	博士 教授	高新院	Sonochemistry-assisted microwave synthesis and optical study of single-crystalline US nanoflowers	Ultrasonics Sonochemistry	2008, 15, 4
11	唐淳 郭万林	博士 教授	高新院	Mechanism for superelongation of carbon nanotubes at high temperatures	Physical Review Letters	2008, 100
12	于培师 郭万林	博士 教授	高新院	The influence of Poisson's ratio on thickness-dependent stress concentration at elliptic holes in elastic plates	International Journal of Fatigue	2008, 30, 1
13	张助华 郭万林	博士 教授	高新院	Freestanding (3,0) boron nitride nanotube: Expected to be stable well over room temperature	Appl. Phys. Lett.	2008, 93
14	张助华 郭万林	博士 教授	高新院	Energy-gap modulation of BN ribbons by transverse electric fields: First-principles calculations	Phys. Rev. B	2008, 77, 7
15	赵军华 郭万林	博士 教授	高新院	Three-parameter approach for elastic-plastic fracture of the semi-elliptical surface crack under tension	International Journal of Mechanical Sciences	2008, 50, 7
16	钟文宇 郭万林	博士后 教授	高新院	Intrinsic aqueduct orifices facilitate K+ channel gating	FEBS Letters	2008, 582
17	周斌 郭万林	博士 教授	高新院	Chemisorption of Hydrogen Molecule on Axially Strained (8, 0) Carbon Nanotube	J. Phys. Chem. C	2008, 112
18	周斌 郭万林	博士 教授	高新院	Chemisorption of hydrogen molecules on carbon nanotubes: charging effect from first-principles calculations	Nanotechnology	2008, 19
19	郭宇锋 郭万林	副教授 教授	高新院	Tuning Field-Induced Energy Gap of Bilayer Graphene via Interlayer Spacing	Applied Physics Letters	2008, 92

序号	作者姓名	职称	单位	论文题目	刊物名称	年卷期
20	郭宇锋 郭万林	副教授 教授	高新院	Interlayer energy-optimum stacking registry for two curved graphene sheets of nanometer dimensions	Molecular Simulation	2008, 34
21	姜云鹏 郭万林	副教授 教授	高新院	Numerical studies on the effective shear modulus of particle reinforced composites with an inhomogeneous inter-phase	Computational Materials Science	2008, 43
22	姜云鹏 杨慧 郭万林	副教授 中级 教授	高新院	Numerical study of the influence of particle-cracking to the damage of MMC by the incremental damage theory	International Journal Of Fatigue	2008, 492
23	刘心声 郭万林	教授 教授	高新院	Robustness of the residue conservation score reflecting both frequencies and physicochemistries	Amino Acids	2008, 34
24	周兴才 刘心声	硕士 教授	高新院	The EM algorithm for the extended finite mixture of the factor analyzers model	Computational Statistics and Data Analysis	2008, 52
25	周兴才 刘心声	硕士 教授	高新院	The Monte Carlo EM method for estimating multinomial probit latent variable models	Computational Statistics	2008, 23
26	马燕芳 刘心声	离校学生 教授	高新院	A Favorable Mechanism for Emergence of Cooperative Behavior	Proceedings of the 6th Conference of Biomathematics会议论文	2008
27	余崇民 郭万林	副教授 教授	高新院	Stress intensity factors for the inner generative crack induced by the out-of-plane stress in front of the main through-the-thickness crack	Acta Mechanica	2008, 200, 1-2
28	余崇民 赵军华 郭万林	副教授 博士 教授	高新院	Three-dimensional stress fields near notches and cracks	International Journal of Fracture	2008, 151, 2
29	戴振东	教授	高新院	非连续约束变结构杆机构机器人：运动与控制的若干仿生基础问题	科学通报	2008,53,1
30	孙久荣 戴振东	教授 教授	高新院	非光滑表面仿生学	自然科学进展	2008,18,6
31	杨志贤 戴振东	博士 教授	高新院	甲虫生物材料的仿生研究进展	复合材料学报	2008,25,2
32	戴振东 张亚锋 梁醒财 孙久荣	教授 硕士 教授 教授	高新院	甲虫鞘翅间的锁合机构、联接力及其表面组织效应	中国科学C	2008,38,6
33	李宏凯 孙久荣 戴振东	博士 教授 教授	高新院	动物运动指令的中枢模式发生器对机器人运动控制的启示	机器人	2008,30,3
34	马光磊 戴振东 谭华	硕士 教授 讲师	高新院	电刺激大壁虎中脑对运动行为影响的研究	长沙航空职业技术学院学报	2008,8,1
35	李宏凯 戴振东 石爱菊 张昊	博士 教授 硕士 讲师	高新院	大壁虎在垂直和水平面上小跑和行走的关节角度观测	科学通报	2008,53,1
36	诸素萍 戴振东	硕士 教授	高新院	边缘检测算子在壁虎脑切片显微图像中的研究	现代电子技术	2008, 273, 10
37	李海鹏 戴振东 谭华 郭策	硕士 教授 讲师 教授	高新院	壁虎动物机器人遥控系统	计算机技术与发展	2008, 18, 8
38	丁红燕 戴振东	博士 教授	高新院	TC11钛合金在人造海水中的腐蚀磨损特性研究	摩擦学学报	2008, 28, 2
39	丁红燕 戴振东 周飞	博士 教授 教授	高新院	LY12微弧氧化膜在不同水溶液中的摩擦学行为	中国有色金属学报	2008, 18, 8

序号	作者姓名	职称	单位	论文题目	刊物名称	年卷期
40	戴振东	教授	高新院	An Irreversible Thermodynamic Theory of Friction and Wear	Science in China D	2008
41	戴振东 张亚锋	教授 硕士	高新院	Coupling between elytra of some beetles: Mechanism, forces and effect of surface texture	Science in China C	2008, 51, 10
42	郭策 戴振东 王文波 孙久荣	教授 教授 讲师 教授	高新院	Biomechanics of Adhesion in ecko's Setae	Proceedings of ISNIT & ISIUS 2008	2008,10
43	Pablo. Perea. goodwyn 王金童 王周义 吉爱红 戴振东	外籍 硕士 硕士 副教授 教授	高新院	Water Striders: The Biomechanics of Water Locomotion and Functional Morphology of the Hydrophobic Surface (Insecta: Hemiptera-Heteroptera)	Journal of Bionic Engineering	2008, 5, 121-126
44	文智平 吉爱红 王金童 戴振东	硕士 教授 硕士 教授	高新院	2-维应变式力传感器的优化设计	传感技术学报	2008, 21, 6
45	Pablo. Perea. goodwyn 王金童 王周义 吉爱红 戴振东	外籍 硕士 硕士 副教授 教授	高新院	An accurate method tlo directly measure water strider's stroke force on the water	Central European Journal of Biology	2008, 3, 3
46	Leonid. Frantsevich 吉爱红 戴振东	外籍 副教授 教授	高新院	Adhesibe properties of the arolium of a lantern-fly, lycorma delicatula	Journal of Insect Physiology	2008, 54, 818-827
47	王文波 戴振东 郭策 谭华 蔡雷 孙久荣	讲师 教授 教授 讲师 硕士 教授	高新院	电刺激大壁虎（Gekko gecko）中脑诱导转向运动的研究	自然科学学报	2008,18,9
48	王文波 戴振东 谭华 郭策 孙久荣	讲师 教授 讲师 教授 教授	高新院	A stereotaxic method and apparatus for the Gekko gecko	Chinese Science Bulletin	2008,53,7
49	瞿志俊 于敏 郭策 戴振东	硕士 副教授 教授 教授	高新院	端面接触磨损试验机的研制	机械工程师	2008,12
50	张昊 戴振东 杨松祥	中级 教授 硕士	高新院	蛇腹鳞的结构特点及其摩擦行为	南京航空航天大学学报	2008, 40, 3
51	代良全 张昊 戴振东	硕士 讲师 教授	高新院	仿壁虎机器人足端工作窘分析及其实现协调运动的步态规划	机器人	2008,30,2

序号	作者姓名	职称	单位	论文题目	刊物名称	年卷期
52	侯　倩 程月华 陆宁云 姜　斌	硕士 助研 副教授 教授	高新院	Study on FDD and FTC of satellite attitude control system based on the effectiveness factor	The 2nd International Symposium on Systems and Control in Aeronautics and Astronautics (ISSCAA 2008)	2008
53	程月华 姜　斌 张　娴	助研 教授 硕士	高新院	A Micro-satellite Attitude System Using Sliding Mode Observer and Sliding Mode Controller with Perturbation Estimation	The 2nd International Symposium on Systems and Control in Aeronautics and Astronautics (ISSCAA 2008)	2008
54	张　娴 程月华 姜　斌	硕士 助研 教授	高新院	基于滑模观测器和变结构控制的小卫星姿态控制系统设计	第27 届中国控制会议	2008
55	方莹 黄护林	硕士 教授	高新院	Simulation of Free Surface MHD-Flow and Heat Transfer Around a Cylinder	Heat Transfer Asian Research	2008, 37, 1
56	张炎 黄护林	硕士 教授	高新院	磁控等离子体对收敛喷管性能的影响	航空动力学报	2008, 23, 6
57	周小明 黄护林	博士 教授	高新院	水平磁场对双层流体热毛细对流的影响	工程热物理学报	2008, 29, 11
58	周小明 黄护林	博士 教授	高新院	磁场对双层流体热毛细对流发展的影响	南京航空航天大学学报	2008, 40, 2
59	张炎 黄护林	硕士 教授	高新院	磁控等离子体对圆管内流动和传热的影响	南京航空航天大学学报	2008, 40, 3
60	李博 黄护林	硕士 教授	高新院	非均匀电导率壁面对磁流体自由表面流动的强化传热数值研究	中国工程热物理学会会议论文	2008
61	周小明 黄护林	博士 教授	高新院	磁场对振荡热毛细对流临界参数的影响	中国工程热物理学会会议论文	2008
62	黄富来 黄护林	硕士 教授	高新院	高超声速化学非平衡流动MHD效应的数值模拟	中国工程热物理学会会议论文	2008
63	周小明 黄护林	博士 教授	高新院	磁场对热毛细对流自由表面的影响	全国博士生论坛（能源与环境领域）会议论文	2008
64	王磊磊 黄护林	博士 教授	高新院	传统散热器采暖房内热环境的实验研究	全国博士生论坛（能源与环境领域）会议论文	2008

Journal of
Computational and Theoretical Nanoscience
Vol. 5, 1372–1376, 2008

Ultrahigh Frequency Longitudinal Oscillators from Single-Walled Carbon Nanotubes

Yitao Dai, Wanlin Guo*, Chun Li, and Chun Tang

Institute of Nano Science, Nanjing University of Aeronautics and Astronautics, Nanjing, 210016, China

The promising application of single-walled carbon nanotubes as ultrahigh frequency longitudinal oscillators is presented in this paper. A short (3, 3) carbon nanotube is considered as an example and its axial oscillation is investigated by the *ab initio* molecular dynamics simulations. The effect of the electromechanical coupling on the frequency-domain characteristic is studied. The variation of the electronic structure induced by the geometry deformation produces the anharmonic behavior of the oscillation, while a strong axial electric field hardly affects the eigenfrequencies. A discrete model is also demonstrated to be efficient to describe this oscillation, though the electromechanical coupling effect can not be taken into account, it can predict the fundamental frequency with an error of 0.8% compared with the result of the *ab initio* molecular dynamics simulation. Additionally, both the discrete model and a continuum hollow rod model are used to predict the fundamental frequencies of the single-walled carbon nanotubes with different lengths and diameters. For a tube shorter than 5 nm, the fundamental frequency is over 1 terahertz.

Keywords: Ultrahigh Frequency Longitudinal Oscillator, Electromechanical Coupling, *Ab initio* Molecular Dynamics, Single-Walled Carbon Nanotube.

1. INTRODUCTION

Recently, continuing efforts have been made to fabricate carbon nanotubes (CNTs) based ultrahigh frequency electromechanical oscillators for their potential applications in nanoscale sensors, actuators, resonators, injectors, motors, engines, filters, memories and switching devices.[1–8] Of special interesting is creating longitudinal oscillators formed by double walled carbon nanotubes (DWCNTs), which are introduced by Zheng[1] and his colleagues in 2002. This kind of oscillator is driven by the interlayer van der Waals force, the frequency is predicted to be at gigahertz region. This simple but valuable idea has received considerable attentions.[4, 6, 7, 9] However, until recently, no practical application is reported mainly because that this oscillation can not maintain for a long time due to the energy dissipation and the lack of suitable energy supply.[7, 9–12] Single-walled carbon nanotubes (SWCNTs) have excellent mechanical properties,[13–15] the frequencies of their axial oscillation modes are reported to be at terahertz (THz) region[16] due to their high Young's modulus. And it has also been reported that they can be significantly stretched by axial electric field.[17, 18] Thus, the high potential of creating ultrahigh frequency longitudinal oscillators by activating the axial vibrations of SWCNTs using axial electric field is unmistakable.

The potential of using SWCNTs in practical high frequency oscillators provides the impetus for the simulation of their performance. As these oscillators can be powered by electric field, and the mechanical behavior of CNTs is coupled with the electronic structure,[19–21] it is necessary to assess the electromechanical coupling effect on the oscillation behavior. In this paper, a short (3, 3) SWCNT is taken as an example and the *ab initio* molecular dynamics (*ab*-MD) simulations are performed to study the influence of external electric field and the electronic structure variation during the oscillation on the frequency-domain characteristic of the CNT. Besides this, as the *ab*-MD method is difficult to deal with large systems, both a discrete model and a continuum hollow rod model are used to predict the frequency-domain characteristic of SWCNTs with different lengths and diameters.

2. COMPUTATIONAL METHOD

In the *ab*-MD simulations, the Restricted Hartree–Fock *ab initio* technique[22–24] is used. In this technique, the positions and velocities of the atoms are predicted by Newton's laws of motion, while the force acting on the atoms are determined by solving the Schrödinger equation

$$H\Psi = E\Psi \tag{1}$$

*Author to whom correspondence should be addressed.

1546-1955/2008/5/1372/005 doi:10.1166/jctn.2008.022

where H is the Hamiltonian operator, E is the total energy of the system, and Ψ is the system wavefunction. Based on the Born–Oppenheimer approximation that the motions of the electrons are decoupled from the motions of the nuclei and the Hartree–Fock approximation that translating a polyelectronic problem into a single electronic problem. So that

$$H_i\Psi_i = \varepsilon_i\Psi_i \tag{2}$$

where H_i is the effective one-electron Hamiltonian, Ψ_i is the ith molecular orbital, and ε_i is the orbital energy of the electron in the orbital Ψ_i. When the linear combination of atomic orbitals (LCAO) assumption is used, $\Psi_i = \sum_\mu C_{\mu i}\phi_\mu$, in which ϕ_μ is the μth atomic orbital and $C_{\mu i}$ is the coefficient. The closed shell model is adopted in present calculations so that the Hartree–Fock equation can be conveniently written as a matrix form, or the Roothaan–Hall equation $FC = SCE$, with the Fock matrix F in the form of Ref. [23]:

$$F_{\mu\nu} = \int d\nu\phi_\mu\left[-\frac{1}{2}\nabla_i^2 - \sum_{A=1}^{M}\frac{Z_A}{r_{iA}}\right]\phi_\nu + \sum_{\lambda=1}^{K}\sum_{\sigma=1}^{K}P_{\lambda\sigma}\left[(\mu\nu \mid \lambda\sigma) - \frac{1}{2}(\mu\lambda \mid \nu\sigma)\right] + V_{\mu\nu} \tag{3}$$

where the first term is the core energy of the system, the second term is the Coulomb and exchange interactions energy. P is the charge density matrix and $P_{\lambda\sigma} = 2\sum_{i=1}^{N/2} c_{\lambda i}c_{\sigma i}\cdot(\mu\nu \mid \lambda\sigma)$, where $(\mu\nu \mid \lambda\sigma)$ are the two-electron integrals that may involve up to four different basis functions (ϕ_μ, ϕ_ν, ϕ_λ, ϕ_σ), which may in turn be located at four different centers. $V_{\mu\nu}$ is the influence of external electric fields, S is the overlap integrals matrix and $S_{\mu\nu} = \int d\nu\phi_\mu\phi_\nu$. C is the coefficient matrix, and E is the orbital energy diagonal matrix. The total electronic energy is obtained by solving the Roothaan–Hall equations, which adopt the self-consistent field (SCF) approach. The total energy and atomic interaction force are also obtained with the electronic energy plus the interaction energy between nuclei. The selected numerical free-atom basis sets (STO-3G) are 2s2p atomic orbitals for carbon atoms, and the relative energies are guaranteed to converge to 10^{-6} Hartree. A time step of 0.2 fs, an initial temperature of 0 K, and the isoenergetic ensemble are adopted for the MD processes. After the *ab*-MD simulations, the time history of the coordinates of carbon atoms are analyzed by the Fast Fourier Transform (FFT) to obtain the frequency-domain characteristic.[25] The sampling interval of the FFT is the same as the time step of the MD simulations.

3. RESULTS AND DISCUSSION

3.1. *Ab*-MD Simulations of the CNT

In the *ab*-MD simulations, in order to reduce the computational requirement, a short (3, 3) CNT with 42 atoms is considered as an example. The geometry structure of the CNT is shown in Figure 1(a). The initial length of the CNT in the released state after an *ab initio* quantum mechanics geometry optimization is 7.114 angstrom. The distances from the central layer to the 1st, 2nd, and 3rd layers shown in Figure 1(a) are 1.27, 2.457, and 3.557 angstrom, respectively. Firstly, the CNT is stretched in the z direction with a deformation of 0.2 angstrom. Then it is released and the *ab*-MD simulation is carried out.

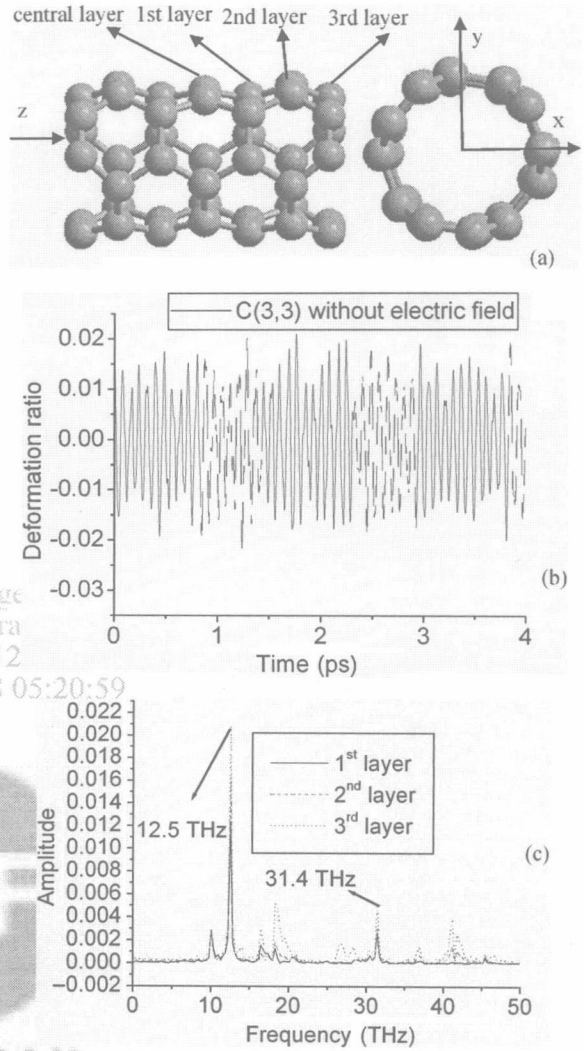

Fig. 1. (a) Atomic model of the freestanding (3, 3) SWCNT considered in the *ab*-MD simulations. (b) Time history of the deformation ratio of the 3rd layer. (c) The oscillation spectrums of the different layers along the axis of the CNT.

Figure 1(b) shows the time history of the deformation ratio of the CNT, where the deformation ratio is defined as the deformation divided by the initial tube length. As the oscillation is anharmonic, the FFT technique is used to get the frequency-domain characteristic. Figure 1(c) shows the oscillation spectrums of the CNT, including all of the three layers along the axis. It is found that, for all of the three layers, there is a peak with the strongest intensity located at 12.5 THz, which is the dominant mode of the

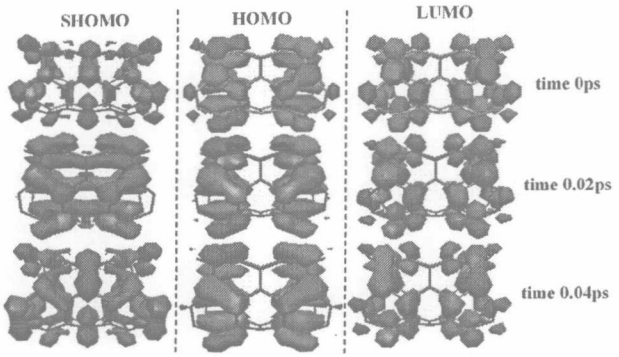

Fig. 2. Electronic structure of the (3, 3) CNT at different periods in the *ab*-MD simulation. From left to right denote to the SHOMO, HOMO, and LUMO, respectively. From top to bottom are the electronic structures of the CNT at the periods when the CNT is under tensile deformation, almost no deformation, and compressive deformation, respectively. The contour value of ploting the molecular orbitals is 0.025.

oscillation. This value is much higher than that of the DWCNT oscillator[1] since the C—C bond interaction is much stronger than the van der Waals interaction between the interlayers. Besides this dominant mode, we also find a second highest peak located at 31.4 THz, which is the second order mode of this oscillation. Corresponding to the anharmonic characteristic of this oscillation, we could find many weak peaks in the spectrum. This anharmonic phenomenon mainly results from the charge density variation during the oscillation.

Figure 2 shows the electronic structure of the CNT at different periods in the *ab*-MD simulation. The highest occupied molecular orbital (HOMO) and the lowest unoccupied molecular orbital (LUMO) almost have no change during the oscillation since they are the orbitals of the dangling bonds, which are only dependent on the structure of the tube end but not sensitive to the axial deformation. The second highest occupied orbital (SHOMO) changes significantly as it is the binding orbital of the CNT that is sensitive to the structure deformation. The variation of binding orbitals will induce a corresponding change of the interaction between the layers, which finally results in the anharmonic oscillation behavior.

To investigate the effect of external electric field on the oscillation behavior, a strong axial electric field with the strength of 0.002 a.u. is applied.

Figure 3 shows the comparison of the oscillation spectrums of the third layer of the CNT with and without external electric field. The unconspicuous change of the spectrum indicates that the existence of electric field almost has no effect on the oscillation. To explain this phenomenon, the electronic structure of the CNT is provided in Figure 4.

No remarkable change can be found for all the SHOMO, HOMO, and LUMO when the axial electric field is applied. Since the mechanical behavior is dependent on the electronic structure, the mechanical oscillation will hardly

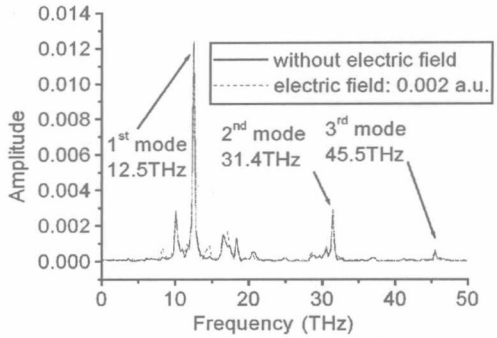

Fig. 3. A comparison of the oscillation spectrums of the CNT with and without electric field.

change its characteristic in this electric field. This result is consistent with the result obtained by density-functional theory in Ref. [19], which reported that when the CNTs are charged with a charge density of 0.6% of the net charge, the shifted range of phonon modes is less than 1%. Here the electronic structure changes slightly when the electric field is applied, so almost no change in the oscillation spectrum can be found.

3.2. Results of Classical Mechanical Models

As the *ab*-MD method is difficult to deal with the system containing a great number of atoms, a discrete model and a continuum hollow rod model are used to study the size effects of the CNTs on the frequency-domain characteristic of these oscillators.

In the discrete model shown in Figure 5(a), the CNT is simplified as an ideal one-dimensional structure with each atom layer being treated as a sphere, and the interactions between adjacent layers are considered as linear springs. The interactions between the nonadjacent layers are ignored as the van der Waals interaction is too small compared with the C—C bonding interaction between the adjacent layers. For a SWCNT fixed at one end, the

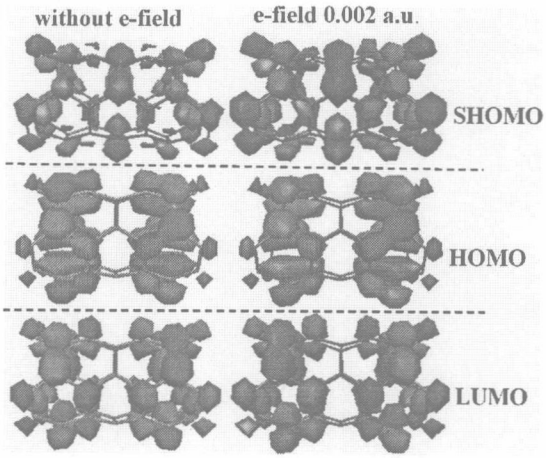

Fig. 4. Electronic structure of the (3, 3) CNT with and without electric field. The contour value of ploting the molecular orbitals is 0.025.

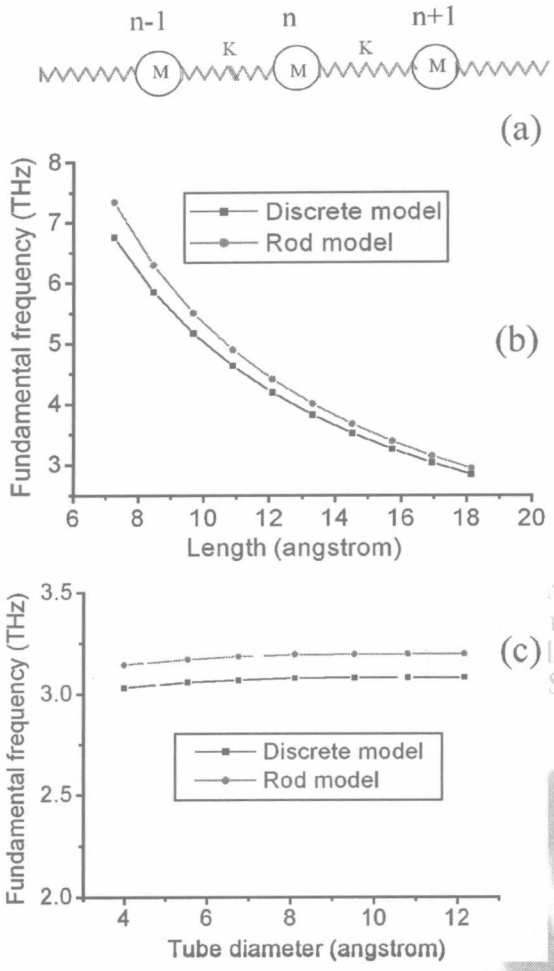

Fig. 5. (a) Discrete model of the SWCNT. (b) Fundamental frequencies of the (3, 3) SWCNTs with different lengths predicted by the discrete model and the rod model. (c) Fundamental frequencies of the armchair CNTs with the length of 1.694 nm.

dynamical behavior of each layer can be described by the equation as follows:

$$\begin{cases} M\ddot{u}_n + K(2u_n - u_{n+1} - u_{n-1}) = 0 \\ M\ddot{u}_N + K(u_N - u_{N-1}) = 0 \\ u_0 = 0 \end{cases} \quad (4)$$

where M is the total mass of a layer, u_0 is the deformation of the fixed layer, u_n $(n = 1, 2, 3, \ldots, N-1)$ is the deformation of the nth layer, and u_N is the deformation of the free layer. The elastic constant K describing the interaction of the adjacent layers can be expressed as $\pi Y_s D/L$, where Y_s and D are the surface Young's modulus, which is defined in Ref. [26], and the diameter of the SWCNT, respectively. L is the distance between the adjacent layers. In the hollow rod model, for a SWCNT with the length of l and fixed at one end, the intrinsic frequency f is given as

$$f = \frac{\pi}{l}\left(r - \frac{1}{2}\right)\sqrt{\frac{Y_s}{\rho_s}} \quad (r = 1, 2, \ldots) \quad (5)$$

Table I. Eigenfrequencies of the CNT shown in Figure 1(a) obtained by the *ab*-MD simulation, the discrete model, and the hollow rod model. Frequencies are in THz.

	Ab-MD	Discrete model	Rod model
1st mode	12.5	12.6	14.9
2nd mode	31.4	34.7	44.9
3rd mode	45.5	50.3	74.9

The surface mass density of the SWCNT ρ_s is defined as $\rho_s = \rho t$, where ρ and t are the volume mass density and the thickness of the hollow rod, respectively. The uses of the surface Young's modulus and surface mass density eliminate the argument of not-well-defined tube thickness.[26] For a (3, 3) SWCNT, the surface Young's modulus is taken as 0.34 (TPa nm).[26] As a comparison, the frequency-domain characteristic of the CNT considered in the *ab*-MD simulation is also studied by both the discrete model and the hollow rod model.

Table I shows the eigenfrequencies of the CNT obtained from different methods. Though the effect induced by the variation of electronic structure can not be considered, compared with the *ab*-MD simulation, the errors of eigenfrequencies obtained by the discrete model are only 0.8%, 10.51% and 10.55% for the lowest mode, second lowest mode, and highest mode, respectively. The corresponding errors of the hollow rod model are much larger than those of the discrete model because the end effect is ignored in this model.

The relationship between the fundamental frequency and the tube length of the (3, 3) SWCNTs fixed at one end is predicted by both the discrete model and the hollow rod model in Figure 5(b). Figure 5(c) shows the fundamental frequencies of the armchair CNTs with the same length of 1.694 nm but different diameters, where the surface Young's modulus of CNTs are taken from Ref. [26]. It is found that the fundamental frequency is reciprocal with the tube length but not sensitive to the tube diameter. This feature can be used for designing SWCNT oscillators with different working frequencies. For instance, the fundamental frequency of a (3, 3) SWCNT shorter than 5 nm can be over 1 THz.

4. CONCLUSIONS

In summary, ultrahigh frequency longitudinal oscillators created by single-walled carbon nanotubes and propelled by axial electric field are introduced. A (3, 3) CNT with the length of 7.114 angstrom is taken as an example and the frequency-domain characteristic is studied by the *ab*-MD simulations. From the present results we draw the following conclusions. (a) The eigenfrequencies of this CNT are over 10 THz, which are much higher than those of the DWCNTs oscillator. (b) The axial deformation during the oscillation will change the binding orbital

of the CNT and finally produces the anharmonic oscillation behaviour. (c) The existence of an axial electric field of 0.002 a.u. is proved to have little effect on the eigenfrequencies for there is almost no polarization of charge density in the CNT under this electric field.

As the *ab*-MD simulations can hardly deal with large systems, a discrete model and a continuum hollow rod model are also used to study the oscillation behaviour of the SWCNTs. Though the electromechanical coupling effect is ignored, the simple discrete model is also demonstrated to be efficient. It can predict the fundamental frequency of the CNT in the *ab*-MD simulations within an error of 0.8%. Furthermore, the size effects of the SWCNTs on the frequency-domain characteristic are predicted by both of the mechanical models. It shows that the fundamental frequency is reciprocal with the tube length but not sensitive to the tube diameter, and for a tube shorter than 5 nm, the fundamental frequency is over 1 THz. This may be useful for controlling the working frequency of the oscillators.

Acknowledgments: The work is supported by National NSF (No.10372044), Jiangsu Province NSF, the Program for Changjiang Scholars and Innovative Research Team in University (PCSIRT) and the Cultivation Fund of the Key Scientific and Technical Innovation Project of the Ministry of Education of China (No.705021).

References

1. Q. Zheng and Q. Jiang, *Phys. Rev. Lett.* 88, 045503 (**2002**).
2. H. B. Peng, C. W. Chang, S. Aloni, T. D. Yuzvinsky, and A. Zettl, *Phys. Rev. Lett.* 97, 087203 (**2006**).
3. P. Poncharal, Z. L. Wang, D. Ugarte, and W. A. De Heer, *Science* 283, 1513 (**1999**).
4. D. Lu, Y. Li, U. Ravaioli, and K. Schulten, *Phys. Rev. Lett.* 95, 246801 (**2005**).
5. L.-H. Wong, Y. Zhao, and G. Chen, *Appl. Phys. Lett.* 88, 183107 (**2006**).
6. J. Kang, K. O. Song, H. J. Hwang, and Q. Jiang, *Nanotechnology* 17, 2250 (**2006**).
7. C. Li and T.-W. Chou, *Appl. Phys. Lett.* 84, 1023 (**2004**).
8. P. Liu, Y. W. Zhang, and C. Lu, *J. Appl. Phys.* 97, 094313 (**2005**).
9. W. Guo, Y. Guo, H. Gao, Q. Zheng, and W. Zhong, *Phys. Rev. Lett.* 91, 125501 (**2003**).
10. X. Zhao and P. T. Cummings, *J. Chem. Phys.* 124, 134705 (**2006**).
11. S. B. Legoas, V. R. Coluci, S. F. Braga, P. Z. Coura, S. O. Dantas, and D. S. Galvão, *Phys. Rev. Lett.* 90, 055504 (**2003**).
12. W. Guo, W. Zhong, Y. Dai, and S. Li, *Phys. Rev. B* 72, 075409 (**2005**).
13. M. M. Treacy, T. W. Ebbesen, and J. M. Gibson, *Nature* 381, 678 (**1996**).
14. A. Rochefort, P. Avouris, F. Lesage, and D. Salahub, *Phys. Rev. B* 60, 13824 (**1999**).
15. G. Gao, T. Çağin, and W. Goddard III, *Nanotechnology* 9, 184, (**1998**).
16. G. Cao, X. Chen, and J. W. Kysar, *Phys. Rev. B* 72, 235404 (**2005**).
17. W. Guo and Y. Guo, *Phys. Rev. Lett.* 91, 115501 (**2003**).
18. I. Cabria, C. Amovilli, M. J. López, N. H. March, and J. A. Alonso, *Phys. Rev. A* 74, 063201 (**2006**).
19. A. Z. Hartman, M. Jouzi, R. L. Barnett, and J. M. Xu, *Phys. Rev. Lett.* 92, 236804 (**2004**).
20. C. Tang, W. Guo, and Y. Guo, *Appl. Phys. Lett.* 88, 243312 (**2006**).
21. Yu. N. Gartstein, A. A. Zakhidov, and R. H. Baughman, *Phys. Rev. B* 68, 115415 (**2003**).
22. Y. Guo and W. Guo, *J. Phys. D* 36, 805 (**2003**).
23. A. R. Leach, Molecular Modelling, Addison Wesley Longman Limited, London (**1996**).
24. I.-F. W. Kuo and C. J. Mundy, *Science* 303, 658 (**2004**).
25. J. M. Seminario, P. A. Derosa, L. E. Cordova, and B. H. Bozard, *IEEE Transactions on Nanotechnology* 3, 215 (**2004**).
26. T. Chang and H. Gao, *Journal of the Mechanics and Physics of Solids* 51, 1059 (**2003**).

Received: 21 May 2007. Accepted: 24 June 2007.

Nano Res (2008) 1: 176–183
DOI 10.1007/s12274-008-8014-7
Research Article

Simulation Studies of a "Nanogun" Based on Carbon Nanotubes

Yitao Dai, Chun Tang, and Wanlin Guo (✉)

Institute of Nano Science, Nanjing University of Aeronautics and Astronautics, Nanjing 210016, China

Received: 3 May 2008/ Revised: 30 June 2008/Accepted: 30 June 2008

ABSTRACT

Quantum mechanical molecular dynamics simulations show that electrically neutral carbon nanotubes or fullerene balls housed in an outer carbon nanotube can be driven into motion by charging the outer tube uniformly. Positively and negatively charged outer tube are found to have quite different actions on the initially neutral nanotubes or fullerene balls. A positively charged tube can drive out the molecule inside it out at speeds over 1 km/s, just like a "nanogun", while a negatively charged tube can drive the molecule into oscillation inside it and can absorb inwards a neutral molecule in the vicinity of its open end, like a "nano-manipulator". The results demonstrate that changing the charge environment in specific ways may open the door to conceptually new nano/molecular electromechanical devices.

KEYWORDS

Energy conversion, carbon nanotube, neutral molecule, driving mechanisms

Introduction

The ability to drive or power functional molecular devices based on unconventional operating principles is of essential interest in various scientific disciplines and technologies [1–5]. A large variety of driving mechanisms have been found by using electromagnetic, electrostatic, or domain-switching principles for devices containing a net charge [6], magnetic moment [7] or electrical domains [8]. Based on such principles, external magnetic or electric fields have been used to provide the driving force. However, neutral molecules have no net charge, magnetic moment or electrical domain, and hence finding a way of driving them remains a challenge [9, 10]. In contrast to artificial systems, biomolecular systems such as protein-motors [11, 12], voltage-gated ion channels [13], and ATP-triggered guest releasers [14] are surprisingly efficient and can work in response to very slight changes in charge [15] or other factors [16].

When size is reduced to the nano or molecular scale, the local fields of matter or structure play an important role, comparable to external fields, and novel driving mechanisms may become dominant. Carbon nanotubes (CNTs) are well known for their exceptional mechanical and electronic properties [17], and recent research has also shown that CNTs and fullerenes are very sensitive to external charge environments or applied fields as the sp^2 carbon atoms have a rich π-electron cloud [18, 19]. High quality multiwalled and biwalled CNTs and CNT structures containing fullerene balls or bamboo sections can be easily fabricated [20, 21]. These carbon structures can be independent and free to move inside a housing nanotube with ultra-low friction [22–

Address correspondence to wlguo@nuaa.edu.cn

24]. The outer tube can be engineered to be open one or both ends, be separate or in bulk films, and also can be fixed to an electrode [24]. Without an applied charge or external field, the core tube or fullerene will remain held in the housing tube by virtue of van der Waals interactions [22].

Here we show by extensive quantum mechanical molecular dynamics simulations on an ideal model that an electrically neutral fullerene ball or carbon nanotube inside an outer housing carbon nanotube can be driven to move when the housing tube is uniformly charged. A positive charge on the house can drive out the neutral core tube or fullerene ball at high speed like a bullet, while a negative charge can drive it to oscillate within the housing tube.

1. Modelling and methods

The typical model considered in this work is a short capped (5, 5) CNT core or a C_{60} molecule in an outer housing (18, 0) CNT with one end capped and the other open. The initial system is firstly optimized by the AMBER molecular mechanics force field, the outer part is then fixed and an energy minimization is performed using the parametrization 3 of the modified neglect of diatomic orbital (PM3) quantum mechanics (QM) method for the inner part. The MM+ molecular mechanics force field (the extension of version 2 of Allinger's molecular mechanics force field) can also be used for the energy minimization of the initial system and no essential difference was found in the subsequent QM simulations. Finally, the outer housing tube is charged with a specific uniform density and the core part is calculated using the QM method to provide the driving force on each atom. Once the energy parameters of the atoms are obtained at one time step, the motion parameters for each atom in the next time step can be determined by Newton' s laws of motion and the velocity and acceleration of the center of mass of the core can be obtained. All the QM molecular dynamics (QMMD) simulations were performed using a Verlet algorithm with a time step of 1 fs at zero initial temperature within a constant energy assumption. The total energies of the whole system are guaranteed to converge to 10^{-5} kcal/mol for all the QM calculations.

In the QMMD simulations, the positions and velocities of the atoms in the system are determined by Newton's laws of motion, while the interactions between the atoms are calculated by solving the Schrödinger equation

$$H\Psi = E\Psi \tag{1}$$

where H is the Hamiltonian operator, E is the total energy of the system, and Ψ is the system wavefunction. The Schrödinger equation is difficult to solve exactly for large molecular systems; however, it is possible to solve the equation in accordance with the Born–Oppenheimer approximation that the motion of the electrons is decoupled from the motion of the nuclei and the Hartree–Fock approximation that a many-electron problem is translated into a single electron problem. Thus,

$$H_i\Psi_i = \varepsilon_i\Psi_i \tag{2}$$

where H_i is an effective one-electron Hamiltonian, Ψ_i is a molecular orbital, and ε_i is the orbital energy of an electron in the orbital Ψ_i. When the linear combination of atomic orbitals (LCAO) assumption is used, $\Psi_i = \sum_{\mu} C_{\mu i}\phi_\mu$ in which ϕ_μ is the μth atomic orbital and $C_{\mu i}$ is the coefficient. The Hartree–Fock (H–F) equation can be conveniently written as a matrix form, or the Roothaan–Hall equation

$$FC = SCE \tag{3}$$

with the Fock matrix F in the form

$$F_{\mu\nu} = \int d\upsilon\, \phi_\mu \left[-\frac{1}{2}\nabla_i^2 - \sum_{A=1}^{M}\frac{Z_A}{r_{iA}}\right]\phi_\upsilon + \sum_{\lambda=1}^{K}\sum_{\sigma=1}^{K} P_{\lambda\sigma}\left[(\mu\upsilon \mid \lambda\sigma) - \frac{1}{2}(\mu\lambda \mid \upsilon\sigma)\right] + V_{\mu\upsilon} \tag{4}$$

where the first term is the core energy, and the second term is the energy arising from the Coulomb and exchange interactions, P is the charge density matrix and $P_{\lambda\sigma} = 2\sum_{i=1}^{N/2} C_{\lambda i}C_{\sigma i}$, $V_{\mu\upsilon}$ represents the influence of external fields, S is the overlap integrals matrix and $S_{\mu\upsilon} = \int d\upsilon\, \phi_\mu \phi_\upsilon$, C is the coefficient matrix, and E is the orbital energy diagonal matrix. $(\mu\upsilon \mid \lambda\sigma)$ and $(\mu\lambda \mid \upsilon\sigma)$ are two-electron integrals that may involve up to four different basis functions (ϕ_μ^A, ϕ_υ^B, ϕ_λ^C, ϕ_σ^D), which may in turn be located at four different centers.

As the whole system contains a large number of atoms and the interaction between the "bullet" and the outer tube housing at the van der Waals distance cannot be described properly by either density

functional theory (DFT) or the Hartree–Fock method [25], a special method called the Mixed Model is used to describe the "nanogun" system. In this method, the outer tube is treated by a classical mechanical model, where the positions and charges of the atoms are fixed and the Slater exponents of s orbitals are used for all the charges; the core part is described by the semi-empirical quantum mechanics method PM3 [26, 27], which considers only the valence electrons of the system and neglects the three- or four-center integrals in the Fock matrix. The interaction between the charges and nuclei of the "bullet" and the housing are considered using the core Hamiltonian correction between the quantum mechanical "bullet" and the classical outer tube housing as follows

$$\Delta H_{\mu\upsilon}=-\sum_{B}(Z_B-Q_B)(\mu_A\upsilon_A\,|s_Bs_B) \tag{5}$$

The interaction energy between the nuclei of the atoms of the "bullet" and all the nuclear and electronic charges on the atoms of the housing is

$$\Delta E=\sum_{(A,B)}\left\{Z_AZ_B(s_As_A\,|s_Bs_B)\left[1+\exp(-\alpha_AR_{AB})+\frac{\exp(-\alpha_AR_{AB})}{R_{AB}}\right]-Z_AQ_B(s_As_A\,|s_Bs_B)\right\} \tag{6}$$

with

$$(s_As_A\,|s_Bs_B)=\left[R_{AB}^2\frac{1}{2}\left(\frac{1}{AM_A}+\frac{1}{AM_B}\right)\right]^{-1/2}$$

where the subscript A represents atoms on the "bullet" and B represents atoms on the housing, s is the s-type orbital, R_{AB} is the distance between atom A and atom B, and AM are the monopole-monopole interaction parameters. Z is the nuclear charge, Q is the electronic charge, and α_A is a monatomic parameter of atom A.

To check the validity of the PM3-based Mixed Model, both H–F ab initio and Kohn–Sham DFT single point calculations were performed on the "nanogun" model used in the PM3 molecular dynamics simulations. Comparison of the calculated dipole moments using the three methods for a C_{60} fullerene "bullet" within a (18, 0) carbon nanotube housing charged with uniform distributed positive charge density of +0.001 e/atom is presented in Fig. 1(a). It can be seen that the variations in dipole moment with position of the "bullet" in the housing show the same trend for all three methods. The curves obtained using the H–F ab initio and the DFT methods are almost the same. The values obtained using the PM3 method are slightly higher, but agree quite well with those of the H–F ab initio and DFT methods. The PM3-based Mixed Model has also been shown to be valid for calculation of the interaction energy. As shown in Fig. 1(b), the variation in the interaction energy of two parallel benzene molecules as a function of separation was calculated and the results compared with those in the literature [28]. The Mixed Model predicts a similar trend to that of the CCSD(T) method, which is thought to be one of the most precise QM methods.

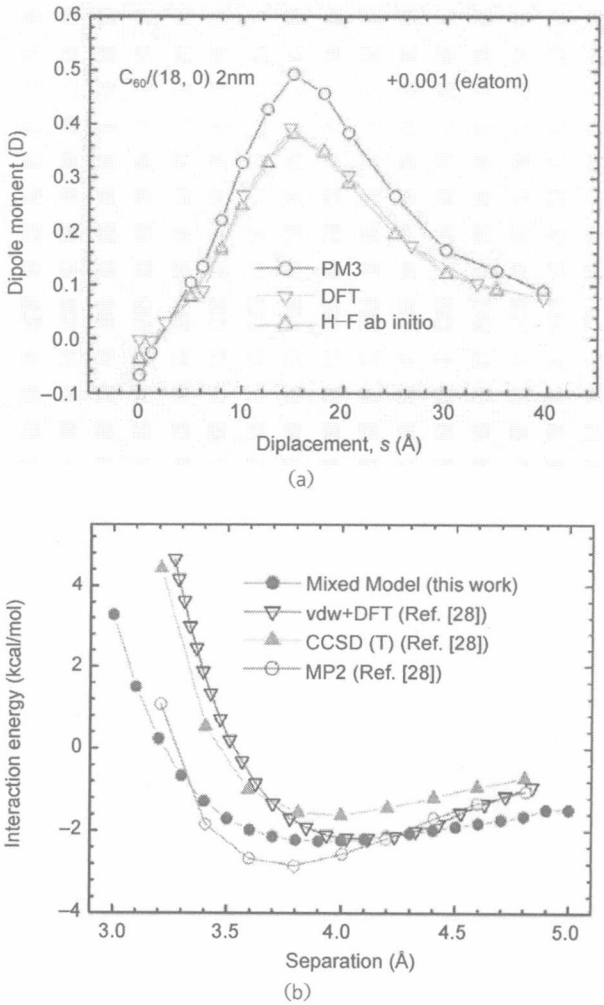

Figure 1 (a) Variation of the dipole moment of the C_{60} "bullet" with its position in the outer (18, 0) tube housing with length of about 2.0 nm. (b) Comparison of the interaction energy between two parallel benzene molecules obtained by the Mixed Model with the results in Ref. [28]

The interaction energy and the dipole moment are directly related to the movement of the core part. The agreement between the interaction energies and the dipole moments with the results obtained by other methods with much higher precision demonstrates that the semiempirical Mixed Model is valid for QMMD simulations of "nano-gun" systems, at least for the models used in this work.

2. Results and discussion

When we charged the housing tube with a positive charge, our QMMD numerical calculations suggested that the encapsulated neutral core tube or fullerene ball can be driven out. A typical total energy curve of a neutral C_{60} molecule moving in a positively charged (18, 0) housing tube with a uniform charge density of 0.001 e/atom is presented in Fig. 2. It can be seen that there are two sharp drops in energy when the fullerene ball leaves the bottom and the open end of the housing tube, while in the middle part of the housing, the energy remains relatively stable. This means that there are two acceleration stages corresponding to the two energy drops which force the ball out. Similar energy curves can be obtained for a CNT core in the charged housing.

Snapshots every 0.5 ps of the driving processes obtained by the QMMD simulations on three typical systems of neutral CNTs or fullerene in charged housing CNTs are shown in Fig. 3(a) with time increasing from top to bottom. In all three cases, the outer tube housings are positively charged with uniform density of +0.001 e/atom. Case A shown in Fig. 3(a) shows a capped (5, 5) core tube with length about 2 nm shooting out from the open end of a fixed (18, 0) housing tube with length about 3.7 nm. Case B in the same figure involves the same core tube in a shorter housing of about 2 nm, and case C involves a neutral C_{60} ball in the 2 nm housing. The speed of ejection of the neutral core in each case is over 1 km/s as shown in Fig. 3(b). Thus, the system resembles a "nanogun" which drives the neutral "bullet" electrically. The velocity curve of the (5, 5) 2 nm/(18, 0) 3.7 nm system (case A) contains four distinct regions: the acceleration region I is the initial stage with a displacement of less than about 0.3 nm, with acceleration up to 2.6×10^{15} m/s^2 and a corresponding driving force of 52 pN/atom; in the following region II, the core tube moves in the housing with relatively stable speed, and when the core reaches the open end of the housing there comes the second acceleration region, region III, with an acceleration of 4.3×10^{14} m/s^2 and driving force of 8.6 pN/atom; when the core is completely out of the outer tube, region IV, the velocity reaches its maximum value of about 1540 m/s. The velocity curve of the C_{60}/(18, 0) 2 nm system (case C) has a similar shape with four regions, while the accelerations in the regions I and III are slightly higher with the maximum final velocity being 1340 m/s. The reason for the lower final velocity of C_{60} is that the acceleration region III is significantly shorter than that available to the 2-nm CNT core. When the outer tube is longer than the core, as in the cases A and C, the two acceleration stages are distinctly separated by a transition region II where the speed is relatively stable. However, when the neutral "bullet" is comparable in length to or longer than the housing, the transition region II disappears and the two acceleration stages merge, as shown in Fig. 3(b) for

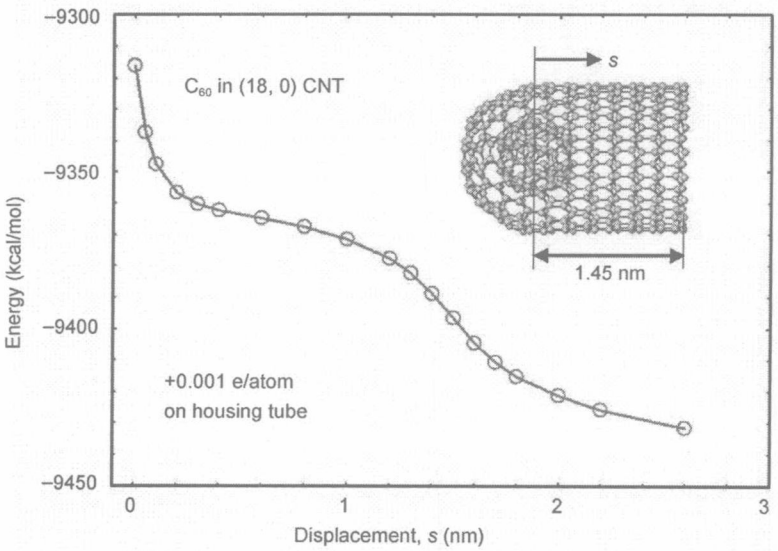

Figure 2 Variation in the energy of the neutral C_{60} ball with its displacement from the bottom of the positively charged (18, 0) CNT housing

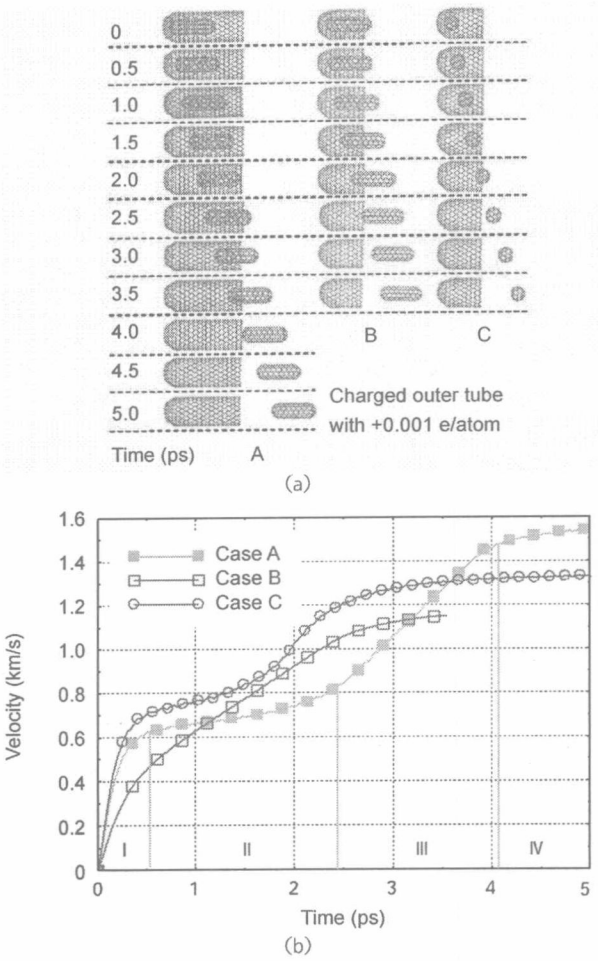

Figure 3 Neutral CNTs or fullerene "bullets" shooting out from positively charged CNT housings with speeds well over 1 km/s. (a) Snapshots of the neutral CNTs or fullerene ball driven out from the open end of the fixed CNT housing by its positive charge. With time increasing from top to bottom, the snapshot interval is 0.5 ps. The density of the charge on the housing is +0.001 e/atom and is evenly distributed. Case A: a capped (5, 5) tube containing 170 atoms with length of about 2.0 nm is shooting out from a fixed (18, 0) tube having 660 atoms and length of about 3.7 nm with one end open; Case B: a capped (5, 5) tube containing 170 atoms with length of about 2.0 nm is shooting out from the open end of a fixed (18, 0) tube having 372 atoms and length of about 2.0 nm; Case C: a C_{60} fullerene ball is shooting out from the open end of a fixed (18, 0) tube having 372 atoms and length about 2.0 nm. (b) The velocity curves of the "bullets" in the three cases

case B in which the "bullet" has the same length as the housing. The accelerations in the merged regions I and III are markedly lower, being 1.3×10^{15} and 3.0×10^{14} m/s^2, respectively. For each of the three cases, the accelerations in stages I and II of the order of 10^{15} and 10^{14} m/s^2, respectively correspond to driving forces on the neutral "bullet" of the order of 1–10 pN/atom, which is about 2 to 3 orders of magnitude higher than the friction force between the core and the housing which is typically 10^{-14} N/atom [22–24]. For a given charge density, the maximum velocity of the neutral "bullet" acquired in the two acceleration stages is dependent on the length of both the housing and bullet.

Increasing the density of the positive charge on the housing tube from +0.001 to +0.005 e/atom monotonically increases the speed of the neutral "bullet" in the (5, 5) 2 nm/(18, 0) 2 nm "nanogun" (case B) from 1150 to about 2200 m/s as shown in Fig. 4(a). Unlike the electrostatic operating principle used in many previous nanodevices [20, 24], the operating mechanism in the present systems is a quantum response of the neutral nanostructure of CNTs or fullerenes to the electrical environment created by the positively charged CNT house. Detailed quantum mechanical analyses show that the "bullet" changes its electronic structure and energy bands, and can be easily polarized in the charged housing; increasing the charge density on the house causes an increase in dipole moment in the "bullet" as shown in Fig. 4(b). For a given positive charge density, the dipole moment first increases and then decreases phase when the "bullet" leaves the housing. Therefore, the driving process is a quantum electrodynamic process. Further numerical calculations demonstrate that a positively charged housing tube with a charge density of +0.001 e/atom can shoot out more than one neutral "bullet" with speeds of over 1 km/s .

For a commensurate set-up of the zigzag housing and zigzag "bullet" system, a positively charged housing CNT can also shoot out the neutral "bullet" at speeds comparable to that of the incommensurate system, as shown in Fig. 4(c). Therefore, the chirality of the system has only a slight effect on the driving process.

Figure 5 shows the different effects of positively and negatively charged housing on a neutral C_{60} ball. It was unexpectedly found that only the positively charged housing tube can drive the ball out, while a negatively charged housing tube only drives the ball into periodic oscillating motion within it. The

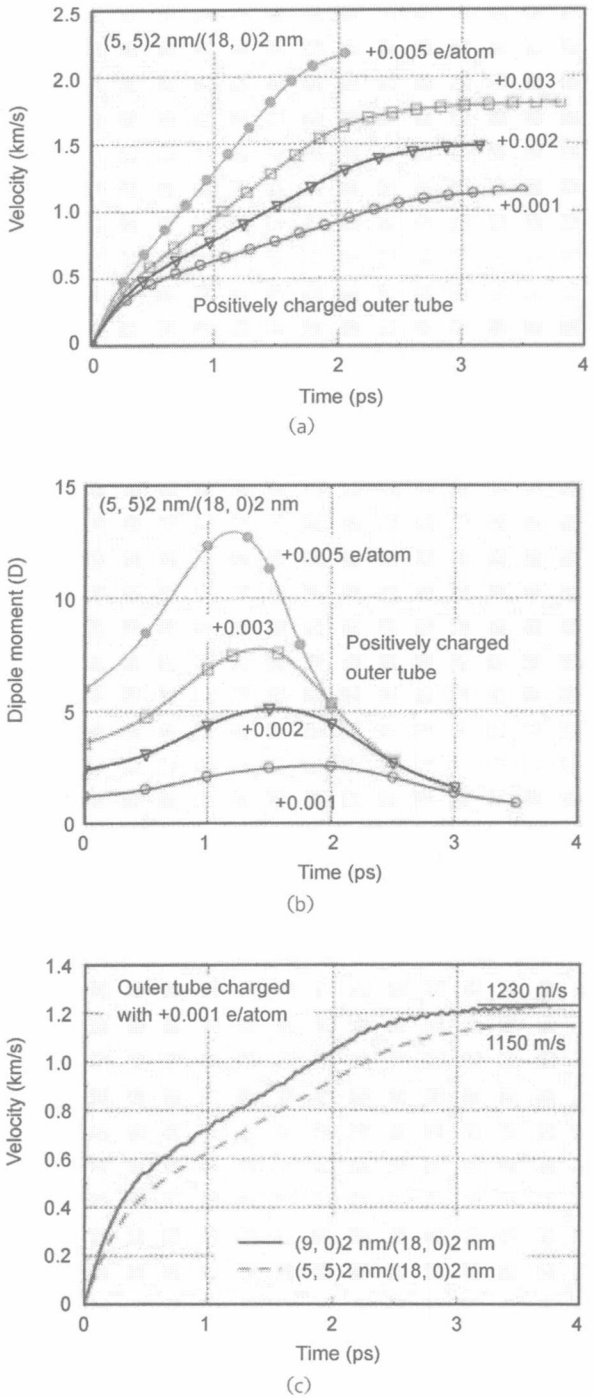

Figure 4 Influence of the charge density on the housing and the chirality of the core tube on the velocity and dipole moment of the neutral "bullets": (a) effect of the density of positive charge on the velocity of the "bullet"; (b) the corresponding dipole moment (in Debye units, D). Increasing the charge density on the housing shell leads to higher dipole moments and higher speeds of the "bullets"; (c) effect of chirality on the velocity of the "bullet"

open end of the negatively charged housing creates a strong force field pushing the ball back inside it and also an absorbing force field in the vicinity of its open end. A fullerene ball put in front of the open end of a negatively charged housing can be absorbed inwards. The inset A in Fig. 5 shows that the ball can achieve inward acceleration in the vicinity of the entrance of the housing tube, except for a very small repulsive region where a slight outward acceleration exists. Therefore, a negative charge can be applied to the housing tube to refill "bullets". This absorbing–releasing cycle can serve as a novel nano manipulation technology. The different charge driving mechanisms operating at the nanoscale can be understood by the asymmetrical response of the electron orbitals to the charged housing environment. As shown in inset B in Fig. 5, when the C_{60} moves along the housing tube, distinct distributions of its highest occupied molecular orbital (HOMO) can be found for the positively and negatively charged

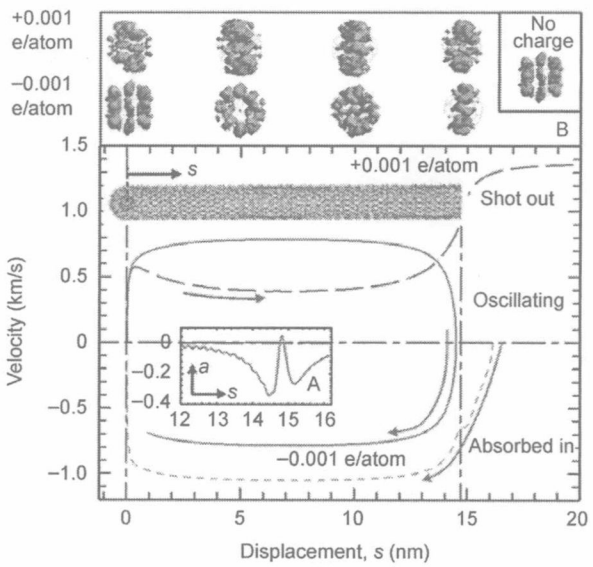

Figure 5 Movement of a C_{60} ball in a long housing (18, 0) tube with positive or negative charge of density of 0.001 e/atom. A C_{60} ball at the bottom (initial s_0=0) of a positively charged tube can be shot out as a "bullet" (blue), while a C_{60} ball at the bottom or in front of the open end (initial s_0=16.1 nm) of a negatively charged tube can be driven into oscillation within the tube (red solid line) or absorbed into the tube (red dashed line). Inset A is the acceleration a (nm/ps^2) of the absorbed C_{60} ball near the entrance of the open end of the housing tube. Inset B shows the variation in the density of the highest occupied molecular orbital (HOMO) of the C_{60} when moving along the housing